RAPID COMMUNICATIONS

PHYSICAL REVIEW FLUIDS **1**, 082403(R) (2016)

Energy spectrum in high-resolution direct numerical simulations of turbulence

Takashi Ishihara
Center for Computational Science, Graduate School of Engineering, Nagoya University, Nagoya 464-8603, Japan

Koji Morishita and Mitsuo Yokokawa
Graduate School of System Informatics, Kobe University, Kobe 657-0013, Japan

Atsuya Uno
RIKEN Advanced Institute for Computational Science, Chuo-ku, Kobe 650-0047, Japan

Yukio Kaneda
Center for General Education, Aichi Institute of Technology, Yakusa-cho, Toyota 470-0392, Japan

(Received 4 September 2016; published 22 December 2016)

A study is made about the energy spectrum $E(k)$ of turbulence on the basis of high-resolution direct numerical simulations (DNSs) of forced incompressible turbulence in a periodic box using a Fourier spectral method with the number of grid points and the Taylor scale Reynolds number R_λ up to $12\,288^3$ and approximately 2300, respectively. The DNS data show that there is a wave-number range (approximately $5 \times 10^{-3} < k\eta < 2 \times 10^{-2}$) in which $E(k)$ fits approximately well to Kolmogorov's $k^{-5/3}$ scaling, where η is the Kolmogorov length scale. However, a close inspection shows that the exponent is a little smaller than $-5/3$, and $E(k)$ in the range fits to $E(k)/[\langle\epsilon\rangle^{2/3}k^{-5/3}] = c(kL)^m$, where $\langle\epsilon\rangle$ is the mean energy dissipation rate per unit mass; L is the integral length scale; and $m \approx -0.12$. The coefficient c is independent of k, but has a R_λ dependence, such as $c = CR_\lambda^\zeta$, where $C \approx 0.9$ and $\zeta \approx 0.14$.

DOI: 10.1103/PhysRevFluids.1.082403

The energy spectrum of turbulence is one of the most fundamental measures characterizing the statistics of turbulent flows. According to the celebrated works by Kolmogorov [1] and Obukhov [2], the energy spectrum $E(k)$ in the so-called inertial subrange $1/\ell_0 \ll k \ll 1/\eta$ of fully developed turbulence at sufficiently high Reynolds number Re far from wall boundaries is given by

$$E(k) = C_K \langle\epsilon\rangle^{2/3} k^{-5/3}, \tag{1}$$

where k is the wave number, C_K is a universal constant, $\langle\epsilon\rangle$ is the mean rate of energy dissipation per unit mass, ℓ_0 is the characteristic length scale of the energy containing eddies, and η is the Kolmogorov micro length scale defined by $\eta \equiv (\nu^3/\langle\epsilon\rangle)^{1/4}$, with ν being the kinematic viscosity.

There have been extensive studies to examine (1). Among them is a study based on a series of high-resolution direct numerical simulations (DNSs) with the number of grid points and the Taylor microscale Reynolds number R_λ up to 4096^3 and approximately 1100, respectively [3]. At relatively low R_λ in the DNS, say up to $R_\lambda < 700$, there is a wave-number range in which the compensated energy spectrum

$$E^C(k) \equiv E(k)/[\langle\epsilon\rangle^{2/3}k^{-5/3}]$$

is fairly flat (i.e., k independent) in agreement with (1), although such a range is not observed in DNSs at very small R_λ (see, e.g., Refs. [4,5]). However, a close inspection of the spectrum at the apparently flat range at $R_\lambda \geqslant 700$ or so showed that $E^C(k)$ is not flat in a strict sense, but a little tilted in the range. The nature of $E(k)$ in such a range remains to be understood.

The main objective of this study is to obtain a better understanding of the k and R_λ dependence of $E(k)$ in such a range at high Re or R_λ in the light of high-resolution DNSs, which we recently performed on the K-computer system at Kobe. The use of the system's 24 576 nodes enabled us to perform DNSs using a Fourier spectral method, with the number of grid points and R_λ up to $12\,288^3$ and approximately 2300, respectively. The readers may refer to Ref. [6] for the parallel computation details.

The numerical method used in the DNSs is basically the same as that used in our previous studies [3,7,8], which is briefly reviewed here for the readers' convenience. The computation domain is assumed to be 2π periodic in each direction of the Cartesian coordinates. Hence, both the minimum wave number $k_{\min}$ and the wave-number increment in the DNSs are unity. The aliasing errors are removed by a phase-shift method. The maximum wave number in each DNS is $k_{\max} = \sqrt{2}N/3$, where N is the number of grid points in each of the Cartesian coordinates in real space. Time marching is accomplished by a fourth-order Runge-Kutta method with a constant time increment Δt. Δt is so chosen that $\Delta t u'/\Delta x < 0.1$ and $\nu k_{\max}^2 \Delta t < 0.02$, in which $\Delta x = 2\pi/N$ and u' is the rms value of the fluctuating velocity in one direction. Double precision arithmetic is used for all the runs.

The total energy $E \equiv 3u'^2/2$ is maintained at an almost time-independent constant ($\approx$0.5) by the introduction of a kind of forcing (a negative viscosity) in the wave-number range $k < K_c$. A similar forcing was used in Refs. [4,9,10]. The variation of the integral length scale L ($\sim \ell_0$) and the eddy turnover time T defined by $L = \pi/(2u'^2)\int_0^k E(k)/k\,dk$ and $T = L/u'$ under this forcing is within 10% of the mean (cf. Ref. [8]).

One of the most important features of high Re turbulence is the wide separation between the wave numbers k_E, where most energy resides, and k_D, where most energy dissipation occurs. Therefore, performing the DNS with k_D/k_E as high as possible is desirable in studying high Re turbulence. However, this is only possible under the following trivial constraint:

$$\frac{k_{\max}}{k_{\min}} = \frac{k_E}{k_{\min}} \times \frac{k_D}{k_E} \times \frac{k_{\max}}{k_D} < \frac{N}{2}. \tag{2}$$

If we define k_D as the wave number, where $k^2E(k)$ takes its maximum, DNSs made so far suggest $k_D\eta \sim c_\eta$, where c_η is generally a constant of order unity and $\sim$0.2 in our DNS. This result implies $k_{\max}/k_D \sim 5k_{\max}\eta$.

The present paper aims to study low-order statistics in the inertial subrange. DNSs made so far suggest that they are not very sensitive to the $k_{\max}\eta$ value, provided that $k_{\max}\eta \gtrsim 1$, although the statistics of higher-order moments may be sensitive to the resolution (see, e.g., Refs. [11–15], the last of which is based on large-scale DNSs with N and R_λ up to 8192 and 1300, respectively). Therefore, we chose ν such that $k_{\max}\eta \sim 1$, which implies $k_{\max}/k_D \sim 5$ in the DNS reported below. The influence of this choice will be addressed again below (Fig. 2). The ratio $k_E/k_{\min}$ in our DNS method is controlled by the constant K_c. We set $K_c = 2.5$ according to our previous studies [3,8]. The readers may refer to Ref. [16] for more details on the implication of constraint (2) and the background idea of using the simple forcing method and periodic boundary conditions.

Table I presents the run conditions and representative turbulence characteristics. The name of each run in column "Run" indicates the N and $k_{\max}\eta$ values. The initial field of each run is provided by the field at the final time step of the run in column "Initial fields." The asterisk denotes the data from our previous DNS [8]. 8192-1† is the field (at $t = 0.6T$) of Run 8192.

Figure 1 presents the time dependence of the normalized dissipation rate $D = \langle\epsilon\rangle L/u'^3$ and $R_\lambda \equiv u'\lambda/\nu$, where $\lambda \equiv (15\nu u'^2/\langle\epsilon\rangle)^{1/2}$. D rapidly changes in an initial transient period at $t/T < 0.5$, but its time dependence is weak after the transient period. $\langle\epsilon\rangle$ denotes a similar time dependence (figure omitted). The results show that $\langle\epsilon\rangle$ does not go to zero with the further increase of Re (see Ref. [3]). The time dependence of R_λ is weak after the transient period. Figure 1 shows that the initial transient period is shorter for runs with a larger N or equivalently larger R_λ. A quantitative idea of the transient period length is obtained by noting that the D value in each run first hits its

TABLE I. DNS conditions and turbulence characteristics at the final time step $t = t_F$.

Run	Initial field	$\mathrm{Re}/10^4$	R_λ	$k_{\max}$	$k_{\max}\eta$	$10^4\Delta t$	$10^5\nu$	$10^2\langle\epsilon\rangle$	L	$10^2\lambda$	$10^4\eta$	T	$10^2\tau_\eta$	t_F
2048-1*	1024-1*	1.61	732	965	1.0	4.0	4.40	7.07	1.23	5.58	10.5	2.13	2.5	$10(4.7T)$
4096-2*	2048-2*	1.37	675	1930	1.9	2.5	4.40	8.31	1.05	5.15	10.1	1.82	2.3	$3.80(2.1T)$
4096-1*	2048-1*	3.65	1131	1930	1.0	2.5	1.73	7.52	1.09	3.39	5.12	1.89	1.52	$4.525(2.4T)$
6144-1	4096-1*	6.35	1423	2896	1.0	1.66	1.02	8.06	1.12	2.51	3.39	1.94	1.17	$3.25(1.7T)$
8192-1	4096-1*	8.97	1747	3862	1.0	1.25	0.70	7.97	1.10	2.10	2.56	1.91	0.94	$2.375(1.2T)$
12288-1	8192-1†	15.4	2297	5793	1.0	0.833	0.41	7.92	1.10	1.62	1.72	1.90	0.72	$1.14(0.6T)$

local maximum at, say, time t_p, then hits its local minimum at, say, time t_b. The time dependence is not very strong after time $t = t_b$. The DNS data show that t_p and t_b fit well to the relations $t_p \approx 25\tau_\eta$ and $t_b \approx 100\tau_\eta$, respectively, where τ_η is the Kolmogorov micro time scale given by $\tau_\eta \equiv (\nu/\langle\epsilon\rangle)^{1/2} \approx \lambda/u' \sim 0.1T/R_\lambda$. In accordance with the previous DNS [8], this result implies that the transient period becomes very short compared to T when R_λ increases.

The resolution level and the simulation time, particularly in the DNSs with high R_λ, are limited by the restriction of the computational resource. It may be worthwhile to obtain some ideas on the potential influence of these limitations on the turbulence statistics before proceeding to the detailed analysis of $E(k)$.

First, let us consider the possible influence of the resolution level (i.e., the choice of $k_{\max}\eta$). Figure 2 illustrates a comparison between $E^C(k)$'s in runs 2048-1 and 4096-2. Both runs are set at $R_\lambda \approx 700$, but with different $k_{\max}$ (i.e., $k_{\max}\eta \sim 1$ in Run 2048-1, and 2 in Run 4096-2). The figure also presents a comparison of energy flux $\Pi(k)$ across k in the two runs. The lines show the spectra averaged over several time steps during $t/T = 1.4$-4.7 for Run 2048-1 and $t/T = 1.1$-2.1 for Run 4096-2. Both of which are after the transition period (i.e., $t > t_b$). Figure 2 also shows the corresponding standard deviations of the spectra as k-dependent shadowed regions. The standard deviations of the spectra are largest near the lower end of k and decrease as k increases.

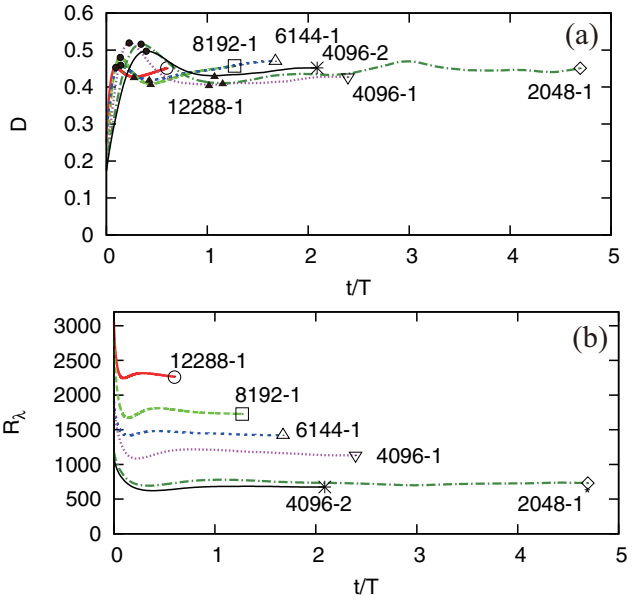

FIG. 1. Time dependence of (a) normalized mean energy dissipation rate $D = \langle\epsilon\rangle L/u'^3$ and (b) Taylor microscale Reynolds number $R_\lambda = \lambda u'/\nu$. •: t_p; ▲: t_b.

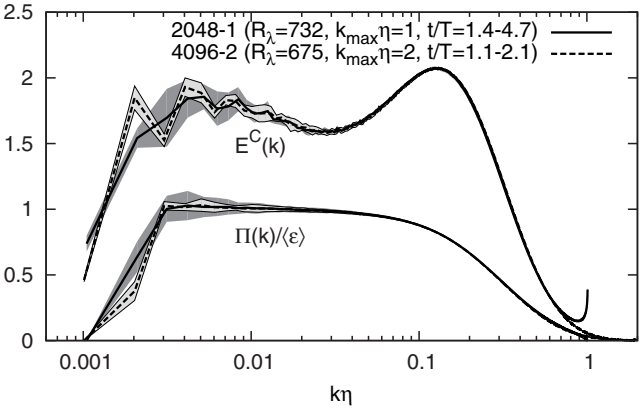

FIG. 2. Compensated energy spectra $E^C(k)$ and normalized energy-flux spectra $\Pi(k)/\langle\epsilon\rangle$ at $R_\lambda \approx 700$ in runs 2048-1 (solid lines) and 4096-2 (broken lines). The lines and shadow regions show, respectively, the averages and standard deviations for both runs taken over several snapshots in the indicated interval.

The averaged energy spectra in runs 2048-1 and 4096-2 are seen to be slightly different from each other in high wave-number range $k\eta \approx 1$ and in low wave-number range ($k\eta < 0.01$). The difference in the ranges is presumably caused by the wave-number truncation at high k and the difference of the energy-containing eddies at the forcing scales. In contrast to the high and low wave-number ranges, the difference between the spectra in the other range ($0.01 < k\eta < 0.8$ in the present case) for the two runs is very small. This observation suggests that the spectrum in the range is insensitive to the difference between $k_{\max}\eta \sim 1$ and $k_{\max}\eta \sim 2$, which is in agreement with the previous studies [11,12]. We shall use the DNS data with $k_{\max}\eta \sim 1$ in the following discussion of the inertial range spectra, unless stated otherwise.

Second, let us consider the possible influence of the simulation time limitation. One might think that the transient effects and time dependence of the statistics may not be negligible if the time is too short. However, as discussed above, Fig. 1 suggests that the initial transient effect or the time dependence is not significant after the transient period $\sim t_b$, at least on one-point statistics, such as on L, D, and $\langle\epsilon\rangle$. However, this does not imply that the influence is also negligible for statistics dominated by very large eddies (i.e., small k range). The influence may be scale or k dependent. Some ideas on the time dependence (or independence) of $E^C(k)$ and $\Pi(k)/\langle\epsilon\rangle$ can be obtained from Fig. 3, which plots the spectra at a few time steps in Run 2048-1. The spectra averaged over the time steps after t_b as well as the corresponding standard deviations are also shown by solid lines and shadow regions, respectively.

The instantaneous energy spectra at different times are seen to be different in Fig. 3, as could be expected, especially at low k. Figure 3 denotes that $E^C(k)$ at low k slowly oscillates in the sense that it goes up and down at an initial stage, and then comes up again. The time period shown in the figure approximately corresponds to the period of one up-and-down cycle. The same is also the case for the energy flux $\Pi(k)$. Therefore, the spectrum is time dependent in a strict sense, especially at low k. However, the time dependence at high k (e.g., $k\eta > 0.01$) is negligibly small in Run 2048-1 after the initial transient period (i.e., at $t > t_b$). These observations suggest that the instantaneous spectra in the high k range are not significantly different from the time-averaged spectra at $t > t_b$. We shall use the spectra averaged over time $t_b < t \leqslant t_F$ of each run in the following, unless stated otherwise.

By the way, as regards the pile-up observed at $k\eta \sim 1$ in Run 2048-1 shown in Fig. 2, one might think that the influence of such a pile-up on $\langle\epsilon\rangle = 2\nu \int k^2 E(k) dk$ may not be negligible. However, according to runs with the same initial condition given by 4096-1* and the same viscosity, but with different resolutions, $k_{\max}\eta \sim 1.5$, 2, and 3, for which $N = 6144$, 8192, and 12 288, respectively, such a pile-up disappears within the time of order τ_η. Moreover, during that time, $\langle\epsilon\rangle$ is almost

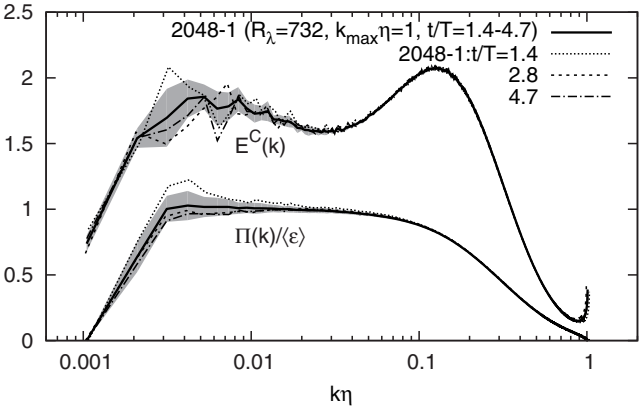

FIG. 3. $E^C(k)$ and $\Pi(k)/\langle\epsilon\rangle$ at $R_\lambda \sim 730$ by Run 2048-1. Solid lines and shadow regions show the average over several snapshots and the standard deviations, respectively. Broken lines show a few snapshot data.

constant (within 0.1%). These runs are short. Hence, they are not included in Table I. This result suggests that the influence of such a pile-up on $\langle\epsilon\rangle$ is small.

Figure 4 illustrates $E^C(k)$ for five runs and suggests that the wave-number range can be divided into three ranges [i.e., F (flat), T (tilted), and B (bump)] given approximately as follows:

$$F = \{k|k\eta \lesssim 5 \times 10^{-3}\},$$
$$T = \{k|5 \times 10^{-3} \lesssim k\eta \lesssim 2 \times 10^{-2}\},$$
$$B = \{k|k\eta \gtrsim 2 \times 10^{-2}\}.$$

In range B, a bump is seen in each curve. The existence of such a bump has been well known in the literature. In accordance with the previous studies [17,18], the bump height in Fig. 4 decreases with the increase in R_λ. Similar bumps are observed in the normalized longitudinal as well as transversal one-dimensional energy spectra. However, they are less prominent than the bump in $E^C(k)$ (figures omitted).

The curves in range T are approximately flat. According to (1), $E^C(k)$ must be a universal constant C_K in the inertial subrange. If the curves were flat (horizontal) in the range, then it is in accordance with K41. However, a close inspection showed that they are not flat in a strict sense, but are slightly tilted in the range. Such a tilt is observed in the DNSs with R_λ up to approximately 1100 [3], as well as in the measurements of atmospheric turbulence [19], turbulence simulations using hyper viscosity [20,21], and large-scale DNSs of turbulence using a forcing method different from that used by the present authors [18,22]. These observations suggest that the tilt is caused by neither an error nor an artifact. A similar tilt is observed in the second-order structure function in the physical space [3].

One might think that such a tilt may be explained by intermittency models, such as Kolmogorov's refined similarity hypothesis called K62 [23] and multifractal models (see, e.g., [24]). According to the models, we have

$$E^C(k) = c_I(kL)^\mu \tag{3}$$

in the inertial subrange, where c_I is a constant independent of ν and k, and μ is a universal constant. Equation (3) motivates us to replot E^C as a function of kL, as shown in Fig. 4(b). As could be expected from Fig. 4(a), the curves in Fig. 4(b) are a little tilted in a certain range of kL (e.g., range T'), which is approximately $kL \sim 30$. The curves in the range are not far from each other. However, the overlap in the range in Fig. 4(b) is worse than that in range T in Fig. 4(a). The same is also the case for the compensated longitudinal and transversal one-dimensional energy spectra (figures

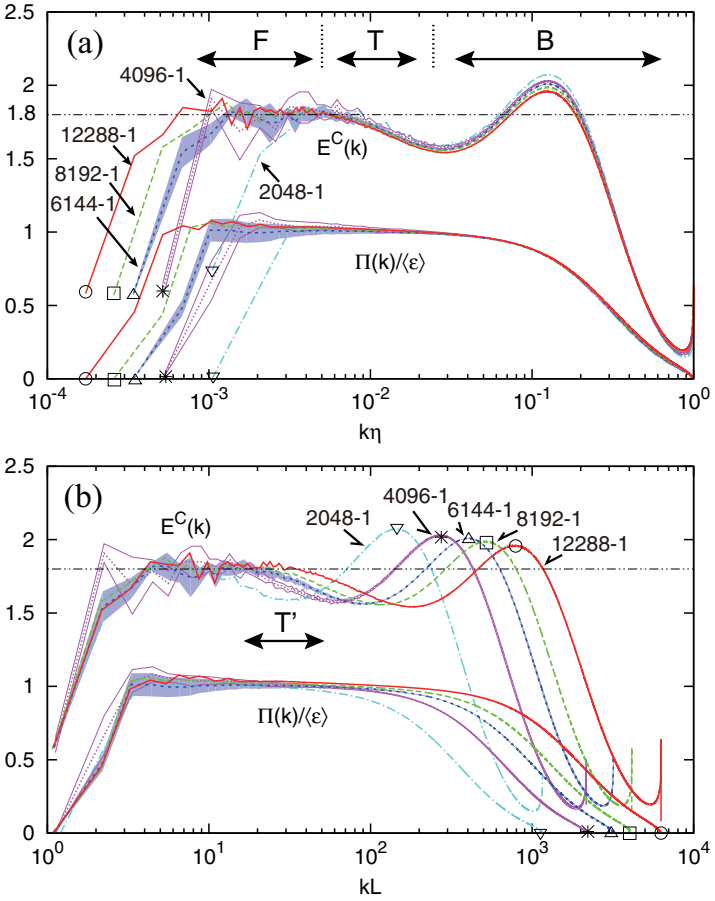

FIG. 4. (a) $E^C(k)$ and $\Pi(k)/\langle\epsilon\rangle$ versus $k\eta$. (b) The same as (a), but versus kL.

omitted). Figure 4(b) presents that $E^C(k)$ in the tilted range (T') depends not only on kL, but also on R_λ. With the increase of R_λ, the curves in T' appear to shift not only upward, but also to the right.

Figure 5(a) indicates the dependence of $E^C(k)$ on R_λ and kL. The two solid lines in the (R_λ,kL) plane show scaling k_pL and $k_bL \propto R_\lambda^{3/2}$, which are derived by assuming $k_p\eta$ and $k_b\eta$ to be independent from R_λ and using the well-known relation $L/\eta \propto R_\lambda^{3/2}$. Figure 5(a) suggests that the curves in the tilted range are approximately on a single plane in the three-dimensional ($\log_{10} kL, \log_{10} R_\lambda, E^C$) space. Let the cross section of this plane and the plane $E^C(k) = \gamma$ be expressed as follows:

$$\log_{10} kL = \alpha \log_{10} R_\lambda + \beta, \quad E^C(k) = \gamma, \tag{4}$$

where α, β, and γ are constants. We acquire the estimates of constants α and β by first setting γ as $\gamma = 1.61, 1.62, \ldots, 1.72$, such that we can identify five points for each of these 12 values for γ, through which the five curves in Fig. 5(a) cross the plane $E^C(k) = \gamma$. We then obtain a set of estimates for α and β by least-squares fitting of (4) to the data of the five points. The 12 sets of (α,β) obtained yields $\alpha = 1.24 \pm 0.03$. Figure 5(a) demonstrates the scaling $kL \propto (R_\lambda)^\alpha$ with $\alpha = 1.24$.

The relation (4) implies that E^C in the tilted range fits well to a function of $X \equiv kL(R_\lambda)^{-\alpha}$. This result is consistent with Fig. 5(b), which displays the plots of $E^C(k)$ vs X with $\alpha = 1.24$. The curves are seen to overlap well in the tilted range, say $0.003 < X < 0.01$. A least square fitting of the data in the range to a straight line $\log_{10} E^C(k) = m \log_{10} X + \log_{10} C$ provides $m = -0.115 \pm 0.005$ and

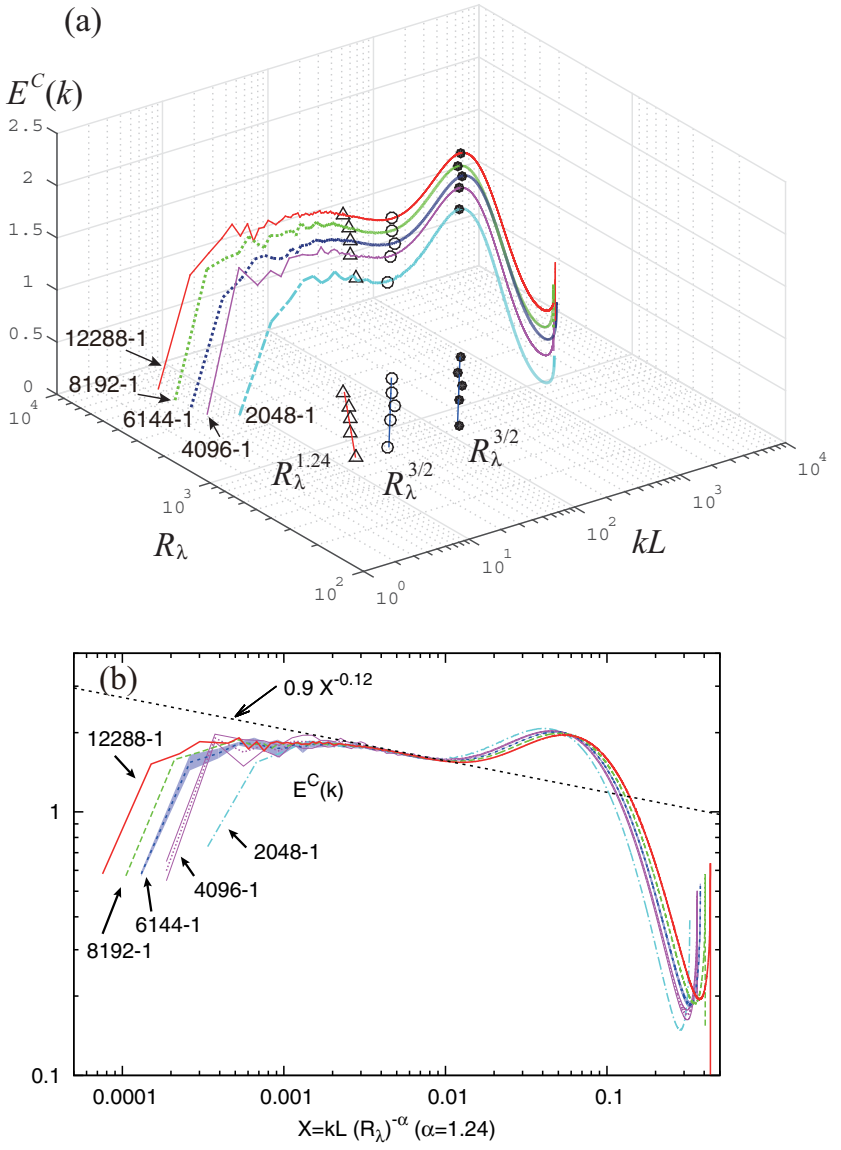

FIG. 5. (a) $E^C(k)$ as a function of kL and R_λ, (b) $E^C(k)$ vs $X = kL(R_\lambda)^{-\alpha}$ with $\alpha = 1.24$. Circles and filled circles show the position of the bump peak k_pL and local minimum k_bL near the bump, respectively. The triangles show the positions of the cross section of the curves with the plane $E^C(k) = 1.70$.

$C = 0.91 \pm 0.03$, which implies

$$E^C(k) = CX^m = c(kL)^m, \tag{5}$$

where $c \equiv C(R_\lambda)^\zeta$ with $\zeta \equiv -\alpha m = 0.14 \pm 0.01$. The relation (5) is shown by the straight dotted line in Fig. 5(b).

The slopes in the tilt ranges of Fig. 4(b) for different runs are not very different from each other. This similarity of slopes for different runs is consistent with the intermittency models such as K62 and fractal models that give (3). However, this slope (given by m) should not be confused with the slope (given by μ) in the theories because the coefficient c in Eq. (5) is R_λ dependent. Therefore, it is

in conflict with the theory (3), in which c_I must be independent of ν or R_λ. The above results suggest that one should be careful in estimating the scaling exponents that are supposed to be relevant for the theories, from the data for the wave-number ranges as high as $k\eta > 5 \times 10^{-3}$. In the physical space, this result implies that one needs to be also careful in estimating the scaling exponents of the structure functions from the data of a small two-point distance. This point will be discussed elsewhere.

According to the models, the constant c_I in Eq. (3) may depend on large-scale flow conditions. Strictly speaking, the possibility that the difference in c for different runs can be explained independently from ν or R_λ is not excluded *a priori*. However, note that the boundary conditions, forcing method, and $k_{\max}\eta$ are the same for the runs studied herein. The expression for c in Eq. (5) is very simple that it appears just natural to assume that c is R_λ dependent. As regards the possibility of R_λ dependence of c in Eq. (5), one may recall the theory by Barenblatt and Goldenfeld, in which c and m may be R_λ dependent [25,26]. However, according to the theory, $m \to 0$ as $R_\lambda \to \infty$, which appears to disagree with m (≈ -0.12) observed in our DNS.

Finally, let us consider range F. The fluctuation in $E^C(k)$ in the range is large, as shown in Fig. 4(a). However, the slope of E^C in F in the figure appears distinctively different from that in T, and $E^C(k)$ looks to be much flatter in the F range than in the T range. Furthermore, the flat-range width increases with R_λ. Such a flat range is too narrow to be identified in DNS if R_λ is too low, say, $R_\lambda \leqslant 700$. The increase in the flat-range width with the increase of R_λ is in accordance with the experiment [19]. The curves for $E^C(k)$ in Fig. 4(a) are not flat in a strict sense. Therefore, how to identify the value of C_K for $E^C(k) = C_K$ from the curves in Fig. 4(a) is not obvious. However, if one uses the range F of Run 6144-1 for the estimate, then one obtains $C_K \sim 1.8 \pm 0.1$. The value is a little higher than the estimates by experiments in the literature (see [27]). The reason behind this, and the question of whether or not range F is the inertial subrange relevant for estimating the exponents in the intermittency models, remain to be explored.

In conclusion, our DNS with R_λ up to 2300 shows among others that, in large-R_λ turbulence, a wave-number range (T range) exists, where the energy spectrum fits well to the power law (5) in k, but the prefactor c depends on R_λ. This finding implies that the statistics in the range are not necessarily free from the viscosity even if the spectrum in a range has a power law dependence on k. As regards the F range, DNSs with larger R_λ and longer simulation time are awaited to examine if there is or there is not any influence on the spectrum in the range by R_λ and/or simulation time.

This study used the computational resources of the K computer provided by the RIKEN Advanced Institute for Computational Science through the HPCI System Research project (Projects ID: hp140135, ID: hp150174, and ID: hp160102). It also used the FX100 system at the Information Technology Center, Nagoya University. This research was partly supported by JSPS KAKENHI Grant Numbers (S) 16H06339, (B) 15H03603, and (C) 26390130.

[1] A. N. Kolmogorov, The local structure of turbulence in incompressible viscous fluid for very large Reynolds numbers, Dokl. Acad. Nauk SSSR **30**, 299 (1941).

[2] A. M. Obukhov, On the distribution of energy in the spectrum of turbulent flow, Dokl. Akad. Nauk SSSR **32**, 22 (1941).

[3] Y. Kaneda, T. Ishihara, M. Yokokawa, K. Itakura, and A. Uno, Energy dissipation rate and energy spectrum in high resolution direct numerical simulations of turbulence in a periodic box, Phys. Fluids **15**, L21 (2003).

[4] J. Jiménez, A. A. Wray, P. G. Saffman, and R. S. Rogallo, The structure of intense vorticity in isotropic turbulence, J. Fluid Mech. **255**, 65 (1993).

[5] P. K. Yeung and Y. Zhou, Universality of the Kolmogorov constant in numerical simulations of turbulence, Phys. Rev. E **56**, 1746 (1997).

[6] K. Morishita, M. Yokokawa, A. Uno, T. Ishihara, and Y. Kaneda, Highly-efficient direct numerical simulation of turbulence by a Fourier spectral method on the K computer, in 27th International Conference on Parallel Computational Fluid Dynamics, Montreal, 2015 (unpublished).

[7] M. Yokokawa, K. Itakura, A. Uno, T. Ishihara, and Y. Kaneda, 16.4-Tflops direct numerical simulation of turbulence by a Fourier spectral method on the Earth Simulator, in *SC '02: Proceedings of the 2002 ACM/IEEE Conference on Supercomputing, Baltimore, 2002* (IEEE Computer Society Press, Los Alamitos, 2002), p. 50.

[8] T. Ishihara, Y. Kaneda, M. Yokokawa, K. Itakura, and A. Uno, Small-scale statistics in high-resolution direct numerical simulation of turbulence: Reynolds number dependence of one-point velocity gradient statistics, J. Fluid Mech. **592**, 335 (2007).

[9] R. M. Kerr, Higher-order derivative correlations and the alignment of small-scale structures in isotropic numerical turbulence, J. Fluid Mech. **153**, 31 (1985).

[10] A. Vincent and M. Meneguzzi, The spatial structure and statistical properties of homogeneous turbulence, J. Fluid Mech. **225**, 1 (1991).

[11] Y. Yamazaki, T. Ishihara, and Y. Kaneda, Effects of wavenumber truncation on high-resolution direct numerical simulation of turbulence, J. Phys. Soc. Jpn. **71**, 777 (2002).

[12] T. Watanabe and T. Gotoh, Inertial-range intermittency and accuracy of direct numerical simulation for turbulence and passive scalar turbulence, J. Fluid Mech. **590**, 117 (2007).

[13] J. Schumacher, Sub-Kolmogorov-scale fluctuations in fluid turbulence, Europhysics Lett. **80**, 54001 (2007).

[14] D. A. Donzis, P. K. Yeung, and K. R. Sreenivasan, Dissipation and enstrophy in isotropic turbulence: Resolution effects and scaling in direct numerical simulations, Phys. Fluids **20**, 045108 (2008).

[15] P. K. Yeung, X. M. Zhai, and K. R. Sreenivasan, Extreme events in computational turbulence, Proc. Natl. Acad. Sci. USA **112**, 12633 (2015).

[16] Y. Kaneda and T. Ishihara, Universality in statistics at small scales of turbulence: A study by high resolution DNS, in *Turbulence and Interactions, Keynote Lectures of the TI 2006 Conference*, Vol. 105, edited by M. Deville, T.-H. Lê, and P. Sagaut (Springer, Berlin, 2009), p. 55.

[17] T. Ishihara, T. Gotoh, and Y. Kaneda, Study of high-Reynolds number isotropic turbulence by direct numerical simulation, Annu. Rev. Fluid Mech. **41**, 165 (2009).

[18] D. A. Donzis and K. R. Sreenivasan, The bottleneck effect and the Kolmogorov constant in isotropic turbulence, J. Fluid Mech. **657**, 171 (2010).

[19] Y. Tsuji, Intermittency effect on energy spectrum in high-Reynolds number turbulence, Phys. Fluids **16**, L43 (2004).

[20] V. Borue and S. A. Orszag, Forced three-dimensional homogeneous turbulence with hyperviscosity, Europhys. Lett. **29**, 687 (1995).

[21] N. E. L. Haugen and A. Brandenburg, Inertial range scaling in numerical turbulence with hyperviscosity, Phys. Rev. E **70**, 026405 (2004).

[22] T. Gotoh and T. Watanabe, Power and Nonpower Laws of Passive Scalar Moments Convected by Isotropic Turbulence, Phys. Rev. Lett. **115**, 114502 (2015).

[23] A. N. Kolmogorov, A refinement of previous hypotheses concerning the local structure of turbulence in a viscous incompressible fluid at high Reynolds number, J. Fluid Mech. **13**, 82 (1962).

[24] U. Frisch, *Turbulence: The Legacy of A. N. Kolmogorov* (Cambridge University Press, Cambridge, 1995).

[25] G. I. Barenblatt and N. Goldenfeld, Does fully developed turbulence exist? Reynolds number independence versus asymptotic covariance, Phys. Fluids **7**, 3078 (1995).

[26] G. I. Barenblatt and A. J. Chorin, Small viscosity asymptotics for the inertial range of local structure and for the wall region of wall-bounded turbulent shear flow, Proc. Natl. Acad. Sci. USA **93**, 6749 (1996).

[27] K. R. Sreenivasan, On the universality of the Kolmogorov constant, Phys. Fluids **7**, 2778 (1995).